



**UNIVERSIDADE ESTADUAL DE CAMPINAS
SISTEMA DE BIBLIOTECAS DA UNICAMP
REPOSITÓRIO DA PRODUÇÃO CIENTÍFICA E INTELECTUAL DA UNICAMP**

Versão do arquivo anexado / Version of attached file:

Versão do Editor / Published Version

Mais informações no site da editora / Further information on publisher's website:

<https://pubs.acs.org/doi/10.1021/acsomega.7b01791>

DOI: 10.1021/acsomega.7b01791

Direitos autorais / Publisher's copyright statement:

©2018 by American Chemical Society . All rights reserved.

DIRETORIA DE TRATAMENTO DA INFORMAÇÃO

Cidade Universitária Zeferino Vaz Barão Geraldo

CEP 13083-970 – Campinas SP

Fone: (19) 3521-6493

<http://www.repositorio.unicamp.br>

Three-Dimensional Superlattice of PbS Quantum Dots in Flakes

Viktor A. Ermakov,^{*,†,‡} José Maria Clemente da Silva Filho,^{†,‡} Luiz Gustavo Bonato,[‡] Naga Vishnu Vardhan Mogili,[§] Fabiano Emmanuel Montoro,[§] Fernando Iikawa,[†] Ana Flavia Nogueira,^{‡,||} Carlos Lenz Cesar,^{†,||} Ernesto Jiménez-Villar,^{†,⊥} and Francisco Chagas Marques[†]

[†]Universidade Estadual de Campinas, IFGW, Campinas, São Paulo 13083-859, Brazil

[‡]Universidade Estadual de Campinas, IQ, Campinas, São Paulo 13083-861, Brazil

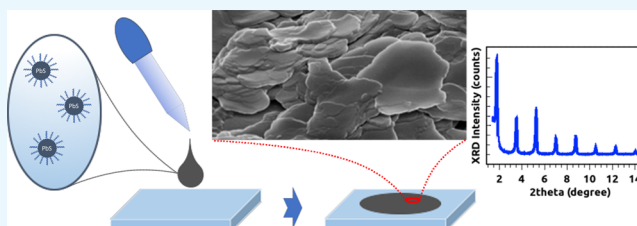
[§]CNPEN, LNNano, Campinas, São Paulo 13083-970, Brazil

^{||}Universidade Federal do Ceará, DF, Fortaleza, Ceará 60440-900, Brazil

[⊥]Instituto de Pesquisas Energéticas e Nucleares, CNEN, São Paulo, São Paulo 05508-000, Brazil

S Supporting Information

ABSTRACT: In the last two decades, many experiments were conducted in self-organization of nanocrystals into two- and three-dimensional (3D) superlattices and the superlattices were synthesized and characterized by different techniques, revealing their unusual properties. Among all characterization techniques, X-ray diffraction (XRD) is the one that has allowed the confirmation of the 3D superlattice formation due to the presence of sharp and intense diffraction peaks. In this work, we study self-organized superlattices of quantum dots of PbS prepared by dropping a monodispersed colloidal solution on a glass substrate at different temperatures. We showed that the intensity of the low-angle XRD peaks depends strongly on the drying time (substrate temperature). We claim that the peaks are originated from the 3D superlattice. Scanning electron microscopy images show that this 3D superlattice (PbS quantum dots) is formed in flake's shape, parallel to the substrate surface and randomly oriented in the perpendicular planes.



INTRODUCTION

Materials with dimensions in the nanometer scale present important changes in their physicochemical properties,^{1–4} being the origin of new phenomena with important applications.^{5–10} More than two decades ago Ashoori¹¹ pronounced a commencement of a new age of science at which structures with essentially atomic properties can be created by humans. The main feature of these structures was a discreet electronic energy spectrum. The “artificial atoms” that he brought to attention are also called quantum dots (QDs). By the analogy with real atoms that can be arranged into a periodic structure forming a crystal, these artificial atoms can also be arranged in so called superlattices.

Simultaneously, with the investigation of properties of single quantum dots, the process of formation of superlattices and their collective properties were studied. In 1995, 1 year before the existence of artificial atoms was declared, Murray et al.¹² reported on the organization of CdSe nanocrystallites into three-dimensional (3D) quantum dot superlattices.

Soon after the pioneering works, it became clear that unlike unorganized particles, nanocrystals arranged into superlattices can have unusual collective properties that were demonstrated on magnetic nanoparticles, where energy exchange in exchange-spring magnets (structures composed of magnetically hard and soft phases) exceeded by over 50% of the predicted theoretical limit.¹³

After more than a decade of the study of superlattices, Nie et al.¹⁴ differentiated four different strategies of the self-assembly of nanoparticles: in solution, using templating methods, at interfaces, and assisted by different factors. Here, in this work, we will focus on the evaporation-induced self-assembly superlattices based on quantum dots at the liquid–solid interfaces.^{15–17} Using this strategy, different types of nanoparticles were organized: 3d-transition metal nanoparticles (Co, Ni, and Fe),^{12,18,19} magnetic,²⁰ and semiconductor.^{14,15,21–23} The superlattices were formed by monodispersed^{12,24} and bidispersed nanoparticles^{15,21–23,25,26} (nanoparticles of two distinct sizes). Recent works conducted by Weidman et al.^{27,28} allowed to see the process of formation of superlattices of PbS monodispersed quantum dots in situ and showed that during this process, different structural transformations can occur.

Similar to atomic crystalline lattices, these superlattices can diffract light with wavelengths comparable with the period of the arrangement of the dots. Quantum dots consist of hundreds of atoms and can have different shapes,^{29,30} as well as their sizes can vary significantly in the range up to 100 nm. Investigation of the superlattices that are formed by nanocrystals with

Received: November 14, 2017

Accepted: February 7, 2018

Published: February 20, 2018

diameters up to 10 nm with conventional X-ray diffraction and scattering techniques (XRD,^{12,22,23,25} small-angle X-ray scattering (SAXS),^{18,19} and grazing-incidence small-angle X-ray scattering (GISAXS)^{24,27–29,31}) that utilize light generated by X-ray tubes (W, Mo, Cu, Ag, Ga, and In) and synchrotron radiation¹⁹ reveal a constructive interference of the light in the region of the low angles up to a few degrees. These peaks that appeared at a specific angular region carry information about the quantum dot arrangement, like interplanar distances and type of crystalline lattice.

Real atoms can form both glassy (amorphous) and crystalline solids, and the crystallization process depends on the cooling rate: lower the rate, higher the level of the crystalline order. By analogy with this natural process, we proposed a hypothesis that for the colloidal quantum dots, the level of organization will depend on the drying time. In this work, by changing the temperature of the substrate and setting the drying time, we show that the intensity of the XRD peaks in the low-degree region increases as the drying time is increased. This reflects the organization of quantum dots. Moreover, the decay rate of the intensity of these peaks as a function of the diffraction angle (order of diffraction) is also indicative of ordering and size of the quantum dots' superlattice size in the direction perpendicular to the sample surface.

EXPERIMENTAL SECTION

Materials. Lead(II) oxide (PbO, yellow powder 99.99%), hexamethyldisilathiane (synthesis grade), trioctylphosphine (90% technical grade), toluene (laboratory reagent, $\geq 99.3\%$), tetrachloroethylene ($>99\%$), chloroform ($\geq 99.8\%$), 1-octadecene (ODE, 90% technical grade), oleic acid (technical grade 90%), and *n*-octane (anhydrous, 99.8%) were purchased by Sigma-Aldrich and used as received.

Synthesis of PbS Nanocrystals. The synthesis of PbS nanocrystal stock solution was performed following a procedure from the literature.³² In a typical synthesis, 360 mg of PbO and 3380 mg of oleic acid were added to 10 mL of 1-octadecene (1-ODE), a non-coordinating solvent, and stirred under vacuum at 110 °C for 6 h, with the formation of a transparent solution. Thereafter, this lead oleate solution was heated until 150 °C and then the solution of sulfur precursor, bis(trimethylsilyl)-sulfide (160 μ L) in 1-ODE (2 mL), was rapidly injected. At this stage, it was observed that there was formation of a dark brown solution, which corresponds to oleic-acid-capped PbS quantum dots. Subsequent to synthesis, the nanocrystals were purified by precipitating in a nonsolvent. This was performed by adding 25 mL of acetone to the reaction product, followed by centrifugation at 12 000 rpm for 5 min. With an aim to remove the excess of oleic acid and impurities, three centrifugation steps were executed. The supernatant was discarded, and the obtained precipitate was dried under nitrogen flow and redispersed in toluene, with a final concentration of 50 mg/mL.²³

Self-Organization of PbS Nanocrystals. The initial colloidal solution of PbS quantum dots in toluene (with a concentration of 50 mg/mL) was precipitated by centrifugation and dried and diluted to 5 mg/mL in *n*-octane, and 100 μ L of the new solution was dropped on round microscopy cover slips (0.17 mm thickness, 24 mm diameter) and placed on hot plates at four different temperatures, room temperature (RT \sim 25 °C), 60, 100, and 140 °C. Because of the different temperatures, the dropped solutions dried for different times: RT, 300 s; 60 °C, 110 s; 100 °C, 50 s; and 140 °C, 45 s. As a

result, grayish black inhomogeneous films were formed on the glass substrates (Figure 1a).

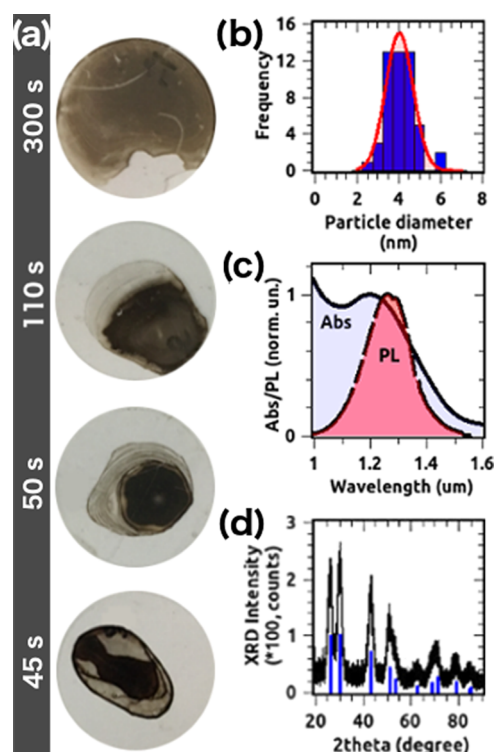


Figure 1. (a) Films of PbS quantum dots, prepared by drop casting of initial solution of quantum dots of PbS and dried at different temperatures; (b) size distribution of nanocrystals; (c) absorption and photoluminescence (PL) spectra of initial solution of PbS quantum dots; (d) XRD pattern of the quantum dots after preparation recorded in 20–90° range (blue lines indicate position and relative intensity of the bulk PbS crystal from ref 34).

Characterization. The PbS quantum dots and the formed films were characterized by means of X-ray diffraction (XRD), scanning electron microscopy (SEM), high-resolution transmission electron microscopy (HR-TEM), absorption, and photoluminescence (PL) spectroscopy.

After preparation of the films of PbS quantum dots, the XRD patterns were recorded in the range of 1–50° using a Rigaku RINR2000 Series diffractometer. SEM was performed on FEI Helios Nanolab 660. HR-TEM analysis was conducted in a TEM-HR Jeol 3010 electron transmission microscope. The microscope was operated at 300 kV, with a point resolution of 0.17 nm. To conduct size distribution analysis of the quantum dots, one separate sample with a lower concentration (less than 0.1 mg/mL) was dropped onto carbon-coated copper grids. A histogram was obtained by a manual measurement of the particle size on bright field TEM images and by automatically counting the particles using free software (Gwyddion and ImageJ). Around 500 particles were analyzed. Absorption spectra were recorded using an Ocean Optics NIRQuest 256 spectrometer. Photoluminescence (PL) measurements were performed using a He–Ne laser (632.8 nm, 1 mW, beam diameter 4 mm) as the excitation light and detected by an Imaging spectrometer iHR320 (Horiba) coupled with a InGaAs-CCD (Andor) cooled by liquid nitrogen (DSS-IGA020L). Room-temperature PL was analyzed from initial

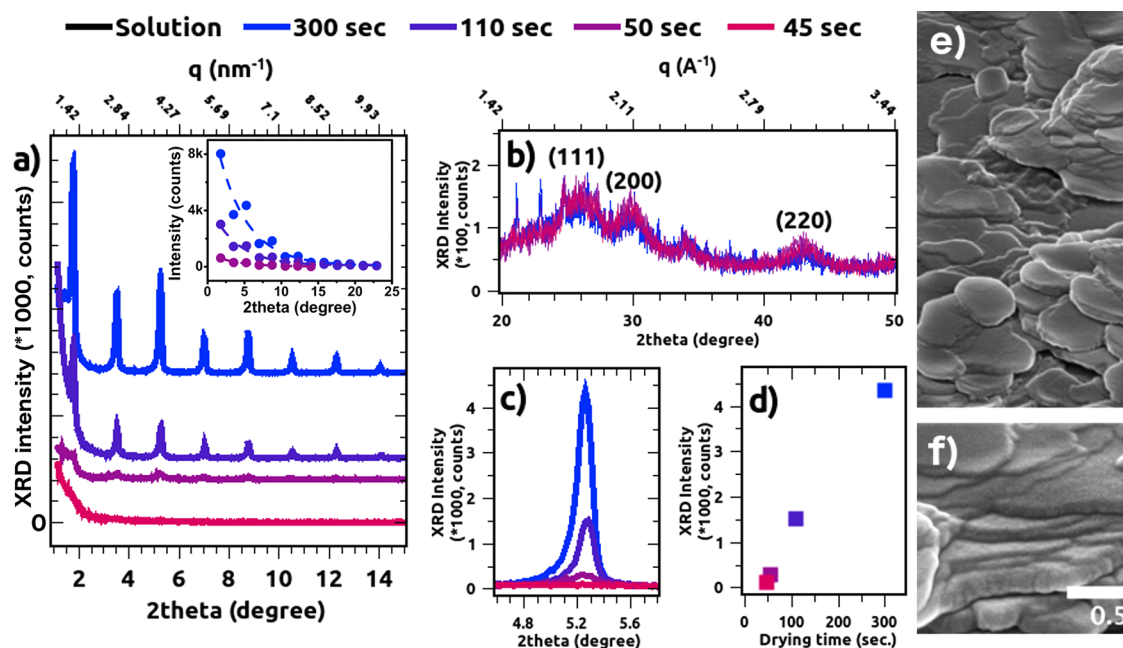


Figure 2. Characterization of organized films of quantum dots: (a) low-angle XRD patterns show an intensity decrease in the peaks associated with arrangement of quantum dots with decrease of drying time (for convenience, XRD patterns are shifted: 300 s, 7000 counts; 110 s, 3000 counts; 50 s, 2000 counts), inset: intensity of the XRD peaks vs peak position (dots) and exponential decay fitting (dashed lines); (b) XRD spectra (20–50°) of the samples show similar intensities of fcc PbS peaks (111), (200), and (220) at different drying times; (c) illustration of the decrease of the 3rd peak at 5.24° (presented in (a)) located at $\sim 5.2^\circ$, with decrease of the drying time; (d) dependence of this 3rd peak on the drying time; (e) SEM image of the sample dried for 300 s, showing formation of the superlattices in the form of flakes randomly oriented in the planes perpendicular to the sample surface; (f) SEM image of the same sample taken at higher magnification; (g) PL spectra of the PbS films show no difference in the position and shape of the PL with decreasing drying time and ~ 100 nm shift compared to that of the initial solution.

colloidal solution of the PbS quantum dots (in a quartz cuvette) and from the dots self-organized on the substrates.

RESULTS AND DISCUSSION

Quantum Dots of PbS. Figure 1b shows the size distribution of the prepared quantum dots revealed by HR-TEM (HR-TEM image of individual quantum dots used to extract size distribution is presented in the Supporting Information). The calculated mode (most frequent) diameter of the nanocrystals was 4.3 nm and experimental data were well fitted by the Gaussian function, with a standard deviation of 0.6 nm (23%).

Figure 1c shows an excitonic peak in the absorption spectrum at 1160 nm and the PL peak at around 1270 nm. The peak in the absorption spectrum confirms the presence of quantum confinement, and in PL spectrum, a stabilization (passivation) of the surface of quantum dots is caused by oleic acid. We also estimated the mean particle diameter using a model proposed by Moreels et al.³³ On the basis of the model, a solution of the equation: $0.0252d^2 + 0.283d - 1/(E_g - 0.41) = 0$ gives the mean diameter d of quantum dots. From the absorption spectrum, we estimated the optical band gap E_g to be 1.07 eV, chose 0.41 eV as a bulk band gap, and solved the equation obtaining the mean diameter to be 3.96 nm, which is in a good agreement with HR-TEM and XRD results.

Figure 1d shows an XRD pattern of the quantum dots, which revealed a PbS face-centered cubic (fcc) arrangement of the lattice. We indexed peaks that correspond to the next planes: 25.99° to (111); 29.89° to (200); 42.90° to (220); 50.50° to (311); 53.30° to (222); 62.30° to (400); 68.40° to (311); 70.30° to (420); 78.60° to (422), and 84.50° to (511). The peaks are in good agreement with the previously reported

values,³⁴ proving the formation of quantum dots of PbS. Using Scherrer's formula,³⁵ with coefficient $K = 0.9$ for spherical particles, we calculated an average size using a width of the (111) and (200) peaks and found that their values are 3.46 and 3.39, respectively, which are about 1 nm less than those found by analyzing TEM images. The reason for this can be explained by the presence of oleic acid molecules (length 1.98 nm) around the dots that provokes an additional contrast on the TEM images increasing the actual size of individual quantum dots.

Films Made from PbS Quantum Dots. Figure 2a shows the low-angle XRD region (up to 15°) of the XRD spectra at which a set of intense sharp peaks spaced at $\sim 1.78^\circ$ are observed for the film prepared at longest drying time, 300 s (Table 1 summarizes the position and relative intensity of observed peaks). The analysis of the position of the peaks reveals that there is only one reflecting plane that results in the

Table 1. Order of Diffraction n , Position $2\theta^\circ$, and Relative Intensity I/I_0 of XRD Peaks Observed for Films of Quantum Dots of PbS

n	position ($2\theta^\circ$)	I/I_0 (%)	n	position ($2\theta^\circ$)	I/I_0 (%)
1	1.78	100	8	14.02	3.9
2	3.5	46.2	9	15.78	3.7
3	5.24	54.3	10	17.56	2.2
4	7	20.5	11	19.32	2.4
5	8.74	22.8	12	21.1	1.1
6	10.5	8.8	13	22.88	1.0
7	12.24	9.2			

formation of the peaks and the positions of the peaks obey Bragg's law $2d \sin \theta = n\lambda$, with increasing order of diffraction n .

These peaks become weaker for the films deposited at shorter time (110 and 55 s) and completely disappear for the film deposited during 45 s. Similar peaks were previously observed for films of PbS quantum dots by Altamura et al.²² and Corricelli et al.^{23,25} and for 4.8 nm (estimated by TEM) CdSe quantum dots.^{12,36} The authors have attributed these peaks to the ordered arrangement of nanocrystals perpendicular to the substrate plane. In our experiment, each film had the same amount of material and the intensity of the peaks of PbS in the region from 20 to 50° remained the same for all four samples, as displayed in Figure 2b. On the basis of these results, we were able to compare the intensity of the low-angle XRD peaks between the samples. The inset in the Figure 2a shows the peak's intensity plotted as a function of the diffraction angle. One can observe that the intensity of the sharp peaks decreases considerably as the drying time decreases, which indicates a lower organization (3D superlattice) in the planes parallel to the substrate surface. The exponential decay fittings ($I(2\theta) = I_0 e^{-\lambda \cdot 2\theta}$, where λ is the exponential decay constant expressed in degree⁻¹) show a quicker decay as the drying time decreases (for the samples found to be $\lambda_{300s} = 3.94$, $\lambda_{110s} = 3.68$, and $\lambda_{50s} = 3.31$). Decrease of the exponential decay rate, λ , indicates that the superlattice organization in the perpendicular direction to the sample surface is also lower as the drying time decreases. We also plotted the 3rd peak at 5.24° for all of the samples (Figure 2c) and show that its intensity monotonically increases with the drying time (Figure 2d).

The spacing (1.78°, 2θ) between these sharp peaks reflects an interplanar distance of 5.02 nm according to Bragg's law ($\lambda_{K\alpha} = 0.15418$ nm, $n = 1$). This distance is different from the size of the quantum dots (estimated by XRD, 3.4 nm), together with the length of the molecule of oleic acid (1.98 nm). Zhrebetskyy et al.³⁷ demonstrated that oleic acid molecule links weakly to the apolar PbS (001) surface by the carboxylic acid group, coordinating the hydrogen on the S^{2-} species and the oxygen on the Pb^{2+} species, whereas the oleate and hydroxylate anions link strongly to the polar PbS (111) by carboxylate groups on the Pb^{2+} species. Thus, the calculated size of the quantum dot together with oleic acid molecule will be 3.4 nm + (2 × 1.98) nm = 7.36 nm, which is much higher than the distance observed by XRD. We can explain this by intercalation of the molecules of oleic acid from the adjacent quantum dots such that the distance between the dots will be calculated as 3.4 nm + (2 × 1.98) nm/2 nm = 5.38 nm. This value is similar to the one retrieved from XRD measurements. Another explanation could be that this difference can be a result of the induced attractive force between the quantum dots, which should predominate over the repulsive force for this short distance (5.02 – 3.40 = 1.62 nm). Thereby, a compression of the oleic acid, placed between QDs, is expected. A similar relation between PbS quantum dot size estimated from Scherrer's formula and a distance calculated from the peak position in SAXS was observed by Baranov et al.³⁸ for the PbS quantum dots with diameter 3.2 nm, interdot spacing was around 5.4 nm. This difference also was attributed to the presence of the oleic acid molecule between quantum dots, whereas the presence of the peak itself was assigned to the quantum dot superlattice.

To observe a constructive interference of X-ray light, the probing system should have reflecting planes perpendicular to the plane formed by the incident and reflected light. From this

perspective, the presence of only one peak attributed to the superlattice, which is a three-dimensional arrangement of the quantum dots and does not look very consistent. To better understand the origin of these peaks, we obtained SEM images of the samples for different drying times. Figure 2e,f shows images of the sample dried for 300 s. SEM images of the samples prepared at lower drying times can be found in the Supporting Information. For the sample dried for 300 s, we observed that quantum dots precipitated in the form of flakes, with a thickness/width ratio higher than 10. These flakes should be oriented randomly in the planes perpendicular to the substrate surface, and formation of such an organized structure may perfectly explain the presence of only one interferential peak in XRD spectra. From the SEM images, we estimated a thickness of the flakes between 20 and 40 nm, which would correspond to 5–8 layers of quantum dots (5–8 sharp peaks in XRD spectra). With decreasing of the drying time, the sizes of flakes decrease and they become fractured, indicating an evidence of diminish in the degree of the quantum dots' organization (see SEM images in the Supporting Information). The precipitation process of PbS QDs should be governed by the increasing of QDs concentration during the drying process, which would provoke the QDs' coalescence and its precipitation onto the substrate surface. Note that the electrostatic and steric forces dominate the stability of colloidal suspension.³⁹ Therefore, a great decrease of the distance between QDs during the drying process must provoke the inductive electrostatic force (attractive) to overcome the steric force, causing the QDs' coalescence. Thereby, the equilibrium between the attractive and repulsive forces between quantum dots determines the formation of the organized lattices similar to the crystal formation.

We paid special attention to the fact that during the formation of quantum dots together with the passivation of dots' surfaces, a separate phase of lead oleate can be formed. In 1949, Vold et al.⁴⁰ showed that during drying of different metal soaps, the metal ions can be arranged in parallel planes separated by a distance somewhat less than twice that of the fatty acid radical that results in the appearance of the X-ray diffraction pattern. Robinet et al. studied lead palmitate, stearate, and oleate phases and showed that a set of sharp peaks appear in their low-angle X-ray pattern.⁴¹ To avoid a possibility for these peaks to be originated from the lead oleate phase, we specially washed a sample four times by centrifugation and separated the precipitated quantum dot phase from the supernatant and redissolved it again in a fresh solvent four times. Also, we separately prepared a solution of lead oleate in *n*-octane and dropped the same amount of it on the glass substrate at RT and at elevated temperatures. We observed a set of sharp peaks similar to that from the literature,⁴¹ but the peaks did not diminish in their intensity when we shortened their drying time, similar to that observed in the X-ray pattern of the quantum dots (from 20 to 50°). We also mentioned that low-angle XRD peaks of lead oleate rapidly disappear with time (1 week) when the sample is stored at RT in the laboratory, whereas peaks of the quantum dot films remain unchanged for months (peaks were repeatedly recorded from the same samples 4 months after the fabrication).

Figure 2g shows PL spectra of the films of PbS quantum dots deposited during different drying times. Even though a significant change in the XRD spectra of the films was observed (Figure 2a,c,d), their PL spectra does not have any notable changes. The shift was only observed between quantum dots in

solution and deposited on a substrate, which is similar to that observed by Choi et al.,⁴² where the authors also showed that the position of the PL peak depends on the distance between dots, and moreover, the exciton dissociation is attributed to the resonant energy transfer rather than to the direct charge transfer. Our results suggest that the average distance between the quantum dots remains approximately the same but the level of organization changes with the drying time.

CONCLUSIONS

We prepared a colloidal solution of PbS quantum dots and deposited it on a glass substrate at different temperatures. We showed that by varying the temperature of the substrate and setting the drying time, we can control the level of the ordering of quantum dots. We associated the intensity of low-angle XRD peaks with the level of ordering and showed that the intensity increases as the drying time is increased. The decay rate of intensity (sharp peaks) as a function of the diffraction angle also indicates the level of ordering in a perpendicular direction to the sample surface, revealing an increase as the drying time increases. SEM images of the films of precipitated PbS quantum dots reveal the formation of flakes in parallel orientation to the sample surface and randomly oriented in perpendicular planes. For the sample dried for 300 s, the thickness of these flakes is estimated between 20 and 40 nm, corresponding to 5–8 layers (PbS quantum dots), which is attributed to the sharp peaks (low-angle XRD) observed with appreciable intensity. PL measurements showed that even though the quantum dots get more organized during longer drying time, the position of their PL peak remains unchanged, suggesting that the proximity between quantum dots is approximately the same. A detailed study of the formation of 3D superlattice, varying the drying time at the same temperature, is necessary to understand better the complex process of ordered precipitation of nanostructures.

ASSOCIATED CONTENT

Supporting Information

The Supporting Information is available free of charge on the ACS Publications website at DOI: 10.1021/acsomega.7b01791.

HR-TEM image of PbS quantum dots; SEM images with different magnifications of samples showing formation of superlattices in the form of flakes (PDF)

AUTHOR INFORMATION

Corresponding Author

*E-mail: victor.ermakov@gmail.com.

ORCID

Viktor A. Ermakov: 0000-0003-1125-4447

José Maria Clemente da Silva Filho: 0000-0003-4110-0609

Ana Flavia Nogueira: 0000-0002-0838-7962

Ernesto Jiménez-Villar: 0000-0002-9049-5881

Author Contributions

All authors contributed to the results analysis of the experiments. V.A.E. and J.M.C.d.S.F. performed the experiments; V.A.E., J.M.C.d.S.F., and E.J.-V. wrote the manuscript. All authors have given approval to the final version of the manuscript.

Notes

The authors declare no competing financial interest.

ACKNOWLEDGMENTS

V.A.E. acknowledges FAPESP (grant 2013/26385-6). J.M.C.d.S.F. acknowledges CNPq (grant 165756/2014-4). E.J.-V. acknowledges FAPESP (grant PV-2017/05854-9). C.L.C. acknowledges the resources obtained from Instituto Nacional de Fotônica Aplicada à Biologia Celular-INFABIC (CNPq grant 573913/2008-0, FAPESP grant 08/57906-3); Biologia das Doenças Neoplásicas da Medula Óssea (FAPESP grant 11/51959-0), and Bolsa de Produtividade (CNPq grant 312049/2014-5) and Centro de Óptica e Fotônica, CEPOF (FAPESP grant 05/51689-2). F.C.M. acknowledges FAPESP (grant 2012/10127-5), INES/INCT/CNPq (grant 465423/2014-0), CNPq (grant 407887/2013-0), CAPES, and Lamult/IFGW/Unicamp.

ABBREVIATIONS

3D, three-dimensional; XRD, X-ray diffraction; SAXS, small-angle X-ray scattering; GISAXS, grazing-incidence small-angle X-ray scattering; (TMS)₂S, hexamethyldisilathiane; TCE, tetrachloroethylene; ODE, 1-octadecene; OLEA, oleic acid; RT, room temperature; SEM, scanning electron microscopy; HR-TEM, high-resolution transmission electron microscopy; TEM, transmission electron microscopy; Abs, absorption; PL, photoluminescent, photoluminescence

REFERENCES

- (1) Alivisatos, A. P. Semiconductor Clusters, Nanocrystals, and Quantum Dots. *Science* **1996**, *271*, 933–937.
- (2) Ermakov, V. A.; Jimenez-Villar, E.; Silva Filho, J. M. C. D.; Yassitepe, E.; Mogili, N. V. V.; Iikawa, F.; de Sá, G. F.; Cesar, C. L.; Marques, F. C. Size Control of Silver-Core/Silica-Shell Nanoparticles Fabricated by Laser-Ablation-Assisted Chemical Reduction. *Langmuir* **2017**, *33*, 2257–2262.
- (3) Fuertes, G.; Sánchez-Muñoz, O. L.; Pedrueza, E.; Abderrafi, K.; Salgado, J.; Jiménez, E. Switchable Bactericidal Effects from Novel Silica-Coated Silver Nanoparticles Mediated by Light Irradiation. *Langmuir* **2011**, *27*, 2826–2833.
- (4) González-Castillo, J. R.; Rodríguez, E.; Jimenez-Villar, E.; Rodríguez, D.; Salomon-García, I.; de Sá, G. F.; García-Fernández, T.; Almeida, D. B.; Cesar, C. L.; Johnes, R.; et al. Synthesis of Ag@Silica Nanoparticles by Assisted Laser Ablation. *Nanoscale Res. Lett.* **2015**, *10*, No. 399.
- (5) Kellermann, G.; Rodríguez, E.; Jimenez, E.; Cesar, C. L.; Barbosa, L. C.; Craievich, A. F. Structure of PbTe(SiO₂)₂/SiO₂ Multilayers Deposited on Si(111). *J. Appl. Crystallogr.* **2010**, *43*, 385–393.
- (6) Jimenez-Villar, E.; Mestre, V.; De Oliveira, P. C.; Faustino, W. M.; Silva, D. S.; De Sá, G. F. TiO₂@Silica Nanoparticles in a Random Laser: Strong Relationship of Silica Shell Thickness on Scattering Medium Properties and Random Laser Performance. *Appl. Phys. Lett.* **2014**, *104*, No. 081909.
- (7) Jimenez-Villar, E.; da Silva, I. F.; Mestre, V.; de Oliveira, P. C.; Faustino, W. M.; de Sá, G. F. Anderson Localization of Light in a Colloidal Suspension (TiO₂@silica). *Nanoscale* **2016**, *8*, 10938–10946.
- (8) Jiménez-Villar, E.; da Silva, I. F.; Mestre, V.; Wetter, N. U.; Lopez, C.; de Oliveira, P. C.; Faustino, W. M.; de Sá, G. F. Random Lasing at Localization Transition in a Colloidal Suspension (TiO₂@Silica). *ACS Omega* **2017**, *2*, 2415–2421.
- (9) Abderrafi, K.; Jiménez, E.; Ben, T.; Molina, S. I.; Ibáñez, R.; Chirvony, V.; Martínez-Pastor, J. P. Production of Nanometer-Size GaAs Nanocrystals by Nanosecond Laser Ablation in Liquid. *J. Nanosci. Nanotechnol.* **2012**, *12*, 6774–6778.
- (10) Popovici, N.; Jimenez, E.; da Silva, R. C.; Branford, W. R.; Cohen, L. F.; Conde, O. Optical and Magnetic Properties of Co-Doped TiO₂ Thin Films Grown by Pulsed Laser Deposition. *J. Non-Cryst. Solids* **2006**, *352*, 1486–1489.

- (11) Ashoori, R. C. Electrons in Artificial Atoms. *Nature* **1996**, 379, 413–419.
- (12) Murray, C. B.; Kagan, C. R.; Bawendi, M. G. Self-Organization of CdSe Nanocrystallites into Three-Dimensional Quantum Dot Superlattices. *Science* **1995**, 270, 1335–1338.
- (13) Zeng, H.; Li, J.; Liu, J. P.; Wang, Z. L.; Sun, S. Exchange-Coupled Nanocomposite Magnets by Nanoparticle Self-Assembly. *Nature* **2002**, 420, 395–398.
- (14) Nie, Z.; Petukhova, A.; Kumacheva, E. Properties and Emerging Applications of Self-Assembled Structures Made from Inorganic Nanoparticles. *Nat. Nanotechnol.* **2010**, 5, 15–25.
- (15) Shevchenko, E. V.; Talapin, D. V.; Kotov, N. A.; O'Brien, S.; Murray, C. B. Structural Diversity in Binary Nanoparticle Superlattices. *Nature* **2006**, 439, 55–59.
- (16) Courty, A.; Mermet, A.; Albouy, P. A.; Duval, E.; Pileni, M. P. Vibrational Coherence of Self-Organized Silver Nanocrystals in F.c.c. Supra-Crystals. *Nat. Mater.* **2005**, 4, 395–398.
- (17) Cheng, W.; Campolongo, M. J.; Cha, J. J.; Tan, S. J.; Umbach, C. C.; Muller, D. A.; Luo, D. Free-Standing Nanoparticle Superlattice Sheets Controlled by DNA. *Nat. Mater.* **2009**, 8, 519–525.
- (18) Murray, C. B.; Sun, S.; Doyle, H.; Betley, T. Monodisperse 3d Transition-Metal (Co,Ni,Fe) Nanoparticles and Their Assembly into Nanoparticle Superlattices. *MRS Bull.* **2001**, 26, 985–991.
- (19) Wang, Z.; Schliehe, C.; Bian, K.; Dale, D.; Bassett, W. A.; Hanrath, T.; Klinke, C.; Weller, H. Correlating Superlattice Polymorphs to Internanoparticle Distance, Packing Density, and Surface Lattice in Assemblies of PbS Nanoparticles. *Nano Lett.* **2013**, 13, 1303–1311.
- (20) Behrens, S. Preparation of Functional Magnetic Nanocomposites and Hybrid Materials: Recent Progress and Future Directions. *Nanoscale* **2011**, 3, 877–892.
- (21) Talapin, D. V.; Shevchenko, E. V.; Bodnarchuk, M. I.; Ye, X.; Chen, J.; Murray, C. B. Quasicrystalline Order in Self-Assembled Binary Nanoparticle Superlattices. *Nature* **2009**, 461, 964–967.
- (22) Altamura, D.; Corricelli, M.; De Caro, L.; Guagliardi, A.; Falqui, A.; Genovese, A.; Nikulin, A. Y.; Curri, M. L.; Striccoli, M.; Giannini, C. Structural Investigation of Three-Dimensional Self-Assembled PbS Binary Superlattices. *Cryst. Growth Des.* **2010**, 10, 3770–3774.
- (23) Corricelli, M.; Altamura, D.; De Caro, L.; Guagliardi, A.; Falqui, A.; Genovese, A.; Agostiano, A.; Giannini, C.; Striccoli, M.; Curri, M. L. Self-Organization of Mono- and Bi-Modal PbS Nanocrystal Populations in Superlattices. *CrystEngComm* **2011**, 13, 3988.
- (24) Weidman, M. C.; Beck, M. E.; Hoffman, R. S.; Prins, F.; Tisdale, W. A. Monodisperse, Air-Stable PbS Nanocrystals via Precursor Stoichiometry Control. *ACS Nano* **2014**, 8, 6363–6371.
- (25) Corricelli, M.; Enrichi, F.; Altamura, D.; De Caro, L.; Giannini, C.; Falqui, A.; Agostiano, A.; Curri, M. L.; Striccoli, M. Near Infrared Emission from Monomodal and Bimodal PbS Nanocrystal Superlattices. *J. Phys. Chem. C* **2012**, 116, 6143–6152.
- (26) Ye, X.; Chen, J.; Diroll, B. T.; Murray, C. B. Tunable Plasmonic Coupling in Self-Assembled Binary Nanocrystal Superlattices Studied by Correlated Optical Microspectrophotometry and Electron Microscopy. *Nano Lett.* **2013**, 13, 1291–1297.
- (27) Weidman, M. C.; Yager, K. G.; Tisdale, W. A. Interparticle Spacing and Structural Ordering in Superlattice PbS Nanocrystal Solids Undergoing Ligand Exchange. *Chem. Mater.* **2015**, 27, 474–482.
- (28) Weidman, M. C.; Smilgies, D.-M.; Tisdale, W. A. Kinetics of the Self-Assembly of Nanocrystal Superlattices Measured by Real-Time in Situ X-Ray Scattering. *Nat. Mater.* **2016**, 15, 775–782.
- (29) Quan, Z.; Fang, J. Superlattices with Non-Spherical Building Blocks. *Nano Today* **2010**, 5, 390–411.
- (30) Quan, Z.; Xu, H.; Wang, C.; Wen, X.; Wang, Y.; Zhu, J.; Li, R.; Sheehan, C. J.; Wang, Z.; Smilgies, D.; et al. Solvent-Mediated Self-Assembly of Nanocube Superlattices. *J. Am. Chem. Soc.* **2014**, 136, 1352–1359.
- (31) Bian, K.; Choi, J. J.; Kaushik, A.; Clancy, P.; Smilgies, D. M.; Hanrath, T. Shape-Anisotropy Driven Symmetry Transformations in Nanocrystal Superlattice Polymorphs. *ACS Nano* **2011**, 5, 2815–2823.
- (32) Hines, M. A.; Scholes, G. D. Colloidal PbS Nanocrystals with Size-Tunable Near-Infrared Emission: Observation of Post-Synthesis Self-Narrowing of the Particle Size Distribution. *Adv. Mater.* **2003**, 15, 1844–1849.
- (33) Moreels, I.; Lambert, K.; Smeets, D.; De Muynck, D.; Nollet, T.; Martins, J. C.; Vanhaecke, F.; Vantomme, A.; Delerue, C.; Allan, G.; et al. Size-Dependent Optical Properties of Colloidal PbS Quantum Dots. *ACS Nano* **2009**, 3, 3023–3030.
- (34) Wyckoff, R. W. G. *Crystal Structures*, 2nd ed.; Wiley: New York, 1963; pp 1–467.
- (35) Langford, J. I.; Wilson, A. J. C. Scherrer after Sixty Years: A Survey and Some New Results in the Determination of Crystallite Size. *J. Appl. Crystallogr.* **1978**, 11, 102–113.
- (36) Murray, C. B.; Kagan, C. R.; Bawendi, M. G. Synthesis and Characterization of Monodisperse Nanocrystals and Close-Packed Nanocrystal Assemblies. *Annu. Rev. Mater. Sci.* **2000**, 30, 545–610.
- (37) Zhrebetskyy, D.; Scheele, M.; Zhang, Y.; Bronstein, N.; Thompson, C.; Britt, D.; Salmeron, M.; Alivisatos, P.; Wang, L.-W. Hydroxylation of the Surface of PbS Nanocrystals Passivated with Oleic Acid. *Science* **2014**, 344, 1380–1384.
- (38) Baranov, A. V.; Ushakova, E. V.; Golubkov, V. V.; Litvin, A. P.; Parfenov, P. S.; Fedorov, A. V.; Berwick, K. Self-Organization of Colloidal PbS Quantum Dots into Highly Ordered Superlattices. *Langmuir* **2015**, 31, 506–513.
- (39) Sánchez-Muñ, O. L.; Salgado, J.; Martínez-Pastor, J.; Jiménez-Villar, E. Synthesis and Physical Stability of Novel Au-Ag@SiO₂ Alloy Nanoparticles. *Nanosci. Nanotechnol.* **2012**, 2, 1–7.
- (40) Hattiangdi, G. S.; Vold, R. D. Characterization of Heavy Metal Soaps by X-Ray Diffraction. *Ind. Eng. Chem.* **1949**, 41, 2311–2320.
- (41) Robinet, L.; Corbeil, M. The Characterization Metal Soaps. *Stud. Conserv.* **2003**, 48, 23–40.
- (42) Choi, J. J.; Luria, J.; Hyun, B.; Bartnik, A. C.; Sun, L.; Lim, Y.; Marohn, J. A.; Wise, F. W.; Hanrath, T. Photogenerated Exciton Dissociation in Highly Coupled Lead Salt Nanocrystal Assemblies. *Nano Lett.* **2010**, 10, 1805–1811.